Applied Physics Letters PERSPECTIVE scitation.org/journal/apl

A Perspective on the optical spectral design for passive solar heating and radiative cooling

Cite as: Appl. Phys. Lett. **121**, 090501 (2022); doi: 10.1063/5.0087687
Submitted: 8 February 2022 · Accepted: 31 July 2022 ·
Published Online: 31 August 2022

Yi Jiang, Jinlei Li, Bin Zhu,[a] and Jia Zhu[a]

AFFILIATIONS

National Laboratory of Solid State Microstructures, College of Engineering and Applied Sciences, Jiangsu Key Laboratory of Artificial Functional Materials, Collaborative Innovation Center of Advanced Microstructures, Frontiers Science Center for Critical Earth Material Cycling, Nanjing University, Nanjing 210093, People's Republic of China

[a]Authors to whom correspondence should be addressed: binzhu@nju.edu.cn and jiazhu@nju.edu.cn

ABSTRACT

Heating and cooling, as the basic requirements of human life, account for more than 28% of global energy consumption. To minimize carbon footprint and save energy, various strategies based on passive heating and cooling have attracted much attention. Typically, as the sun and outer space are the natural thermodynamic resources for renewable energy harvesting, passive solar heating and radiative cooling have been widely explored through a precise spectral design to effectively exploit solar energy and thermal radiation. In this Perspective, based on the previous works and principal development of passive solar heating and radiative cooling, the corresponding ideal spectral design under different temperature conditions is proposed and highlighted. As demonstrations, we present several examples of different optical spectral designs for realizing passive solar heating and radiative cooling to fit various scenarios. Finally, possible solutions to the current problems and the directions for future development are discussed.

I. INTRODUCTION

Heating and cooling based on the traditional methods account for 28% of global energy consumption.[1,2] Therefore, reducing reliance on energy-inefficient heating and cooling methods has a large impact on the global energy landscape. As the sun (~5700 K) and outer space (~3 K) serve as the natural heat source and cold source for renewable energy harvesting,[3] passive solar heating and radiative cooling become the promising strategies for saving energy and minimizing carbon footprint.[4] They have shown great potentials for applications in various scenarios, such as building,[5–9] vapor generation,[10,11] and personal thermal management.[12,13] To efficiently utilize the heat/cold energy from the Sun/outer space, it is crucial to have precise spectral designs in response to the sunlight and thermal radiation under various scenarios.

First, considering a traditional material's surface whose emissivity, $\varepsilon(\lambda,\ \theta)$, is a function of wavelength and angle, when the surface is exposed under the direct sunlight, the net energy input/output per unit area P_{net} can be expressed as

$$P_{net} = P_{solar} + P_{ambient} + P_{surface} + P_{conduction-convection}, \quad (1)$$

where P_{solar} is the power absorbed by the surface from the solar radiation, $P_{ambient}$ is the power absorbed by the surface from the atmosphere thermal radiation, $P_{surface}$ is the power radiated out to the outer space from the surface, and $P_{conduction-convection}$ is the power caused by conduction and convection. We take the energy input as positive and the energy output as negative.

In Eq. (1), the above four energy flows can be further written as

$$P_{solar} = \cos\theta \int I_{AM1.5}(\lambda,\ \theta)\varepsilon(\lambda,\theta)d\lambda, \quad (2)$$

$$P_{ambient} = \int d\Omega \cos\theta \int I_{BB}(T_{ambient},\lambda)\varepsilon(\lambda,\theta)\varepsilon_{ambient}(\lambda,\theta)d\lambda, \quad (3)$$

$$P_{surface} = \int d\Omega \cos\theta \int I_{BB}\left(T_{surface},\lambda\right)\varepsilon(\lambda,\theta)d\lambda, \quad (4)$$

$$P_{conduction-convection} = h_c(T_{ambient} - T_{surface}), \quad (5)$$

where θ is the angle between the direction of incident sunlight and the normal direction of the surface, $I_{AM1.5}(\lambda,\theta)$ is the energy distribution under the solar illumination of the AM1.5 spectrum, $\int d\Omega = 2\pi\int_0^{\pi/2}\sin\theta d\theta$ is the angular integral over a hemisphere, $I_{BB}(T,\lambda) = \frac{2hc^2}{\lambda^5}\frac{1}{e^{hc/\lambda k_B T}-1}$ is the energy distribution under the radiation spectrum of a blackbody at a given temperature T, where h is the Planck's constant, c is the speed of light, k_B is the Boltzmann constant,

and $\varepsilon_{ambient}(\lambda,\theta) = 1 - t(\lambda)^{1/\cos\theta}$ is the emissivity of atmosphere as a function of wavelength and angle, where $t(\lambda)$ is the atmosphere transmittance in the zenith direction,[14] h_c is the collective non-radiative heat coefficient of the surface, $T_{ambient}$ is the ambient temperature, and $T_{surface}$ is the temperature of the surface.

It is clear that to realize efficient passive solar heating or radiative cooling, we must make $P_{net} > 0$ or $P_{net} < 0$, respectively. Specifically, special attention must be paid to the solar spectrum (0.3–2.5 μm) and the middle infrared band (MIR band, 2.5–20 μm) [Fig. 1(a)]. For different temperature conditions of detailed application scenarios, the requirements for spectrum are quite different. In this Perspective, we start by introducing ideal spectra for different conditions in Sec. II. In Sec. III, some specific examples of passive solar heating and radiative cooling applied in different scenarios are presented. In Sec. IV, we discuss the possible solutions to current problems and the directions for future development.

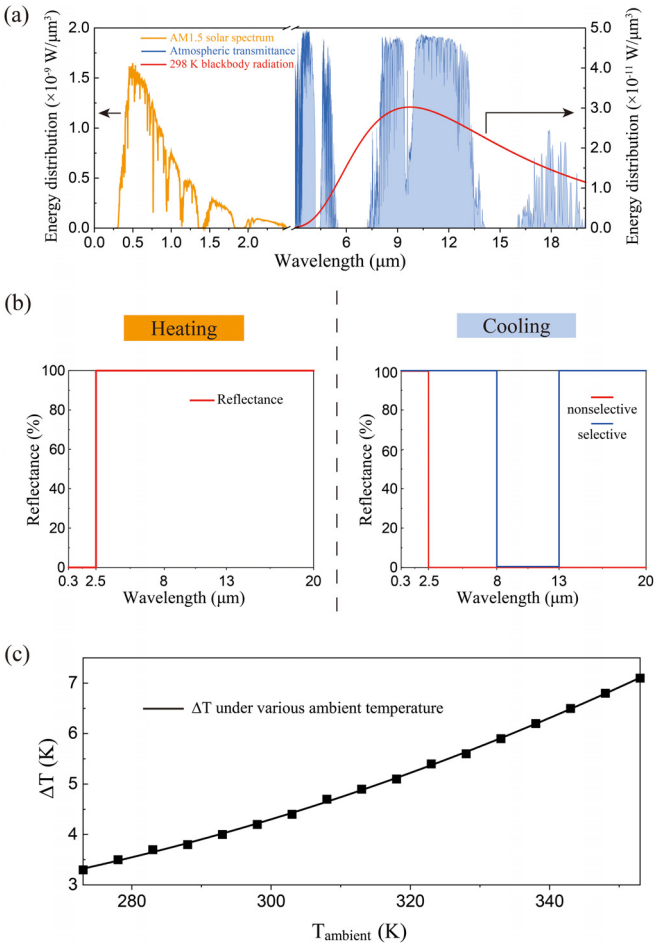

FIG. 1. (a) Energy distribution of the AM1.5 solar spectrum (yellow), blackbody radiation spectrum at 298 K (red), and atmospheric transmittance (blue). (b) Spectrum design of optimal heating (left) and cooling (right) effect in different conditions. When $T_{surface} > T_{ambient} - \Delta T$, nonselective spectrum (red) can have optimal cooling performance. When $T_{surface} < T_{ambient} - \Delta T$, selective spectrum (blue) can have optimal cooling performance. (c) The relationship between ΔT and $T_{ambient}$.

II. IDEAL SPECTRA FOR DIFFERENT TEMPERATURE CONDITIONS

Previous reviews have covered the exciting progress of passive solar heating[15–18] and radiative cooling,[19–22] but the detailed discussion about the specific spectral requirements under the different conditions is not systematically summarized and analyzed. Here, we provide a comprehensive classification on ideal spectra for optimal performance. Assuming that the power caused by conduction and convection is not considered, the boundary conditions of classification are closely linked to utilization of sunlight and radiation exchange between atmosphere and surface. Utilization of sunlight depends on the implemented functions such as heating or cooling, while radiation exchange depends on difference on ambient temperature and surface temperature in an equilibrium state. At a given ambient temperature, there is a turning point of temperature difference ΔT between atmosphere and surface that makes spectral type with optimal cooling effect different,[23,24] where ΔT is a function of $T_{ambient}$ calculated based on the parameter of atmospheric transmittance in the MIR band. [Assume that $1 - \varepsilon_{ambient}(\lambda,\theta)$ is the blue curve in the wavelength range of 2.5–20 μm, as shown in Figs. 1(a) and 1(b).]

If an optimal heating effect needs to be achieved, it is important to have high absorption in the solar spectrum at first. Since the absorption coefficient of materials is generally higher than that of the air, the surface temperature of materials will not be lower than the ambient temperature. Thus, it needs low emissivity in the MIR band in order to minimize its own thermal radiation [Fig. 1(b), left].

If an optimal cooling effect needs to be achieved, the surface must satisfy high reflection in the solar spectrum and high emission in the atmospheric window between 8 and 13 μm. It is worth noting that when $T_{surface} > T_{ambient} - \Delta T$, the thermal radiation can still transfer from surface to ambient via the other MIR band (2.5–8 and 13–20 μm). In summary, the surface must satisfy high reflection in the solar spectrum and high emissivity in the whole MIR band which is also called nonselective spectrum, in order to reflect external heat input as much as possible and maximize own thermal radiation, respectively. When $T_{surface} < T_{ambient} - \Delta T$, the surface must satisfy high reflection in both solar spectrum and MIR band outside the atmospheric window band (8–13 μm) which is called as selective spectrum so that the ambient will not radiate energy to the surface [Fig. 1(b), right].

Based on formula (3) and (4) above, we can figure out the relationship between ΔT and $T_{ambient}$, as shown in Fig. 1(c). We calculate ΔT with an accuracy of 0.1 K under varied $T_{ambient}$ from 273 to 353 K with an interval of 5 K.

III. DETAILED EXAMPLES OF VARIOUS SPECTRA AND MATERIALS

Below we would introduce some specific examples with various spectral and material designs, mainly from our research group, to realize high-performing passive solar heating and radiative cooling.

Interfacial solar vapor generation that localized the absorbed solar at the interface of water and air is introduced as a typical application of passive solar heating. Such a burgeoning technique has been widely applied for enhancing evaporation in various fields, such as desalination,[25,26] wastewater treatment,[27,28] and power generation.[29,30]

In the early work, our group focused on solving the problem of high absorption in the solar spectrum by plasmonic absorbers and carbon-based absorbers. In 2016, Zhou *et al.* achieved high-efficient, broadband absorption in the solar spectrum through self-assembly of metallic nanoparticles on nanoporous alumina template by physical vapor deposition [Fig. 2(a)].[31] They attained the three-dimensional compact arrangement of Au nanoparticles with randomly size distribution in anodic alumina (AAO) template. Due to the randomly

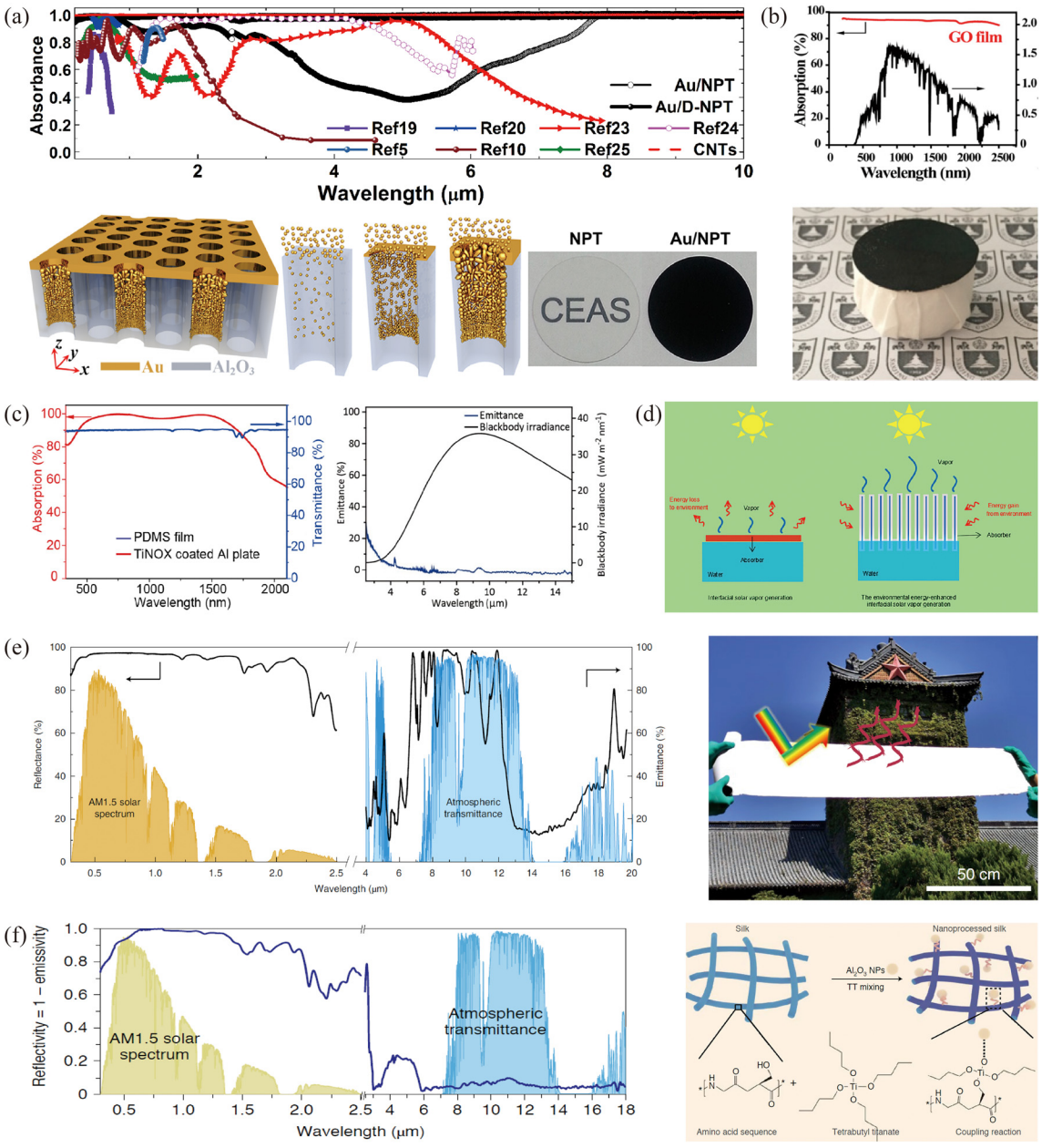

FIG. 2. (a) Absorbance spectrum, schematic diagram, and photograph of Au in the nanoporous template AAO. Reproduced with permission from Zhou *et al.*, Sci. Adv. **2**(4), e1501227 (2016).[31] Copyright 2016 The American Association for the Advancement of Science. (b) Absorption spectrum and optical image of the composite layered structure with graphene oxide and polystyrene foam. Reproduced with permission from Li *et al.*, Proc. Natl. Acad. Sci. **113**(49), 13953 (2016).[34] Copyright 2016 National Academy of Sciences. (c) Spectrum of the selective absorber TiNOX-coated aluminum plate. Reproduced with permission from Wang *et al.*, Joule **5**(6), 1602 (2021).[37] Copyright 2021 Elsevier. (d) Comparison between interfacial solar vapor generation and environmental energy-enhanced interfacial solar vapor generation. Reproduced with permission from Li *et al.*, Joule **2**(7), 1331 (2018).[38] Copyright 2018 Elsevier. (e) Spectral UV–visible–infrared emittance and photograph of the es-PEO film. Reproduced with permission from Li *et al.*, Nat. Nanotechnol. **16**(2), 153 (2021).[39] Copyright 2021 Nature Publishing Group. (f) Spectral UV–visible–infrared emittance and preparation progress of a nanoprocessed silk. Reproduced with permission from Zhu *et al.*, Nat. Nanotechnol. **16**(12), 1342 (2021).[40] Copyright 2021 Nature Publishing Group.

distributed gold nanoparticles with different sizes, the hybridized localized surface plasmon resonance was effectively enhanced so that it could absorb light in a wide wavelength range rather than narrow band absorption in the visible band. Moreover, nanoporous alumina could afford impedance match between absorber and air to reduce the energy loss of reflection and exploit internal trap effect to enhance light absorption. As a result, this absorber achieved absorption more than 99% in the broad wavelength range from 0.4 to 10 μm. Subsequently, in order to reduce the material cost, Zhou *et al.* replaced Au nanoparticles with Al nanoparticles but still ensured 96% absorption in the solar spectrum of 0.3–2.5 μm.[32] Based on the above works, in 2017, they also fabricated spectrum selective plasmonic absorbers with flexibly tuned bandwidth and cutoff wavelength,[33] which provided an idea for coordinated regulation of the solar spectrum and MIR band.

The carbon-based material system also provides high absorption in the solar spectrum through rapid thermalization of electron–electron scattering. In 2016, Li *et al.* prepared the composite layered structure with graphene oxide (GO) and polystyrene foam, achieving 94% sunlight absorption [Fig. 2(b)].[34] This as-prepared design made the foam float above the water and the GO absorber was on the top of the foam which was not in the direct contact with water. It significantly reduced the heat conduction from absorber to water without the influence on the ability of pumping water to the surface. Finally, it achieved energy transfer efficiency of 80% and four orders salinity decrement. In 2017, Hu *et al.* demonstrated a GO-based aerogel with 92% absorption of sunlight and 83% energy transfer efficiency under one-sun illumination on the basis of the carbon-based material.[35] The porous property of the aerogel not only provided the water transport path but also greatly reduced heat loss, which met the requirement of interfacial heating material by only using one material. In addition, Xu *et al.* utilized carbonized mushrooms which had natural artificial transpiration structure and achieved high sunlight absorption.[36] This idea of bionics provided a solution for acquisition of water resource.

Recently, the optimal solar heating effect close to the ideal spectrum has been explored. It needs to regulate emissivity in the MIR band on the basis of high absorption in the solar spectrum. In 2020, Wang *et al.* found a commercially available TiNOX-coated aluminum plate as a selective solar absorber.[37] It had high solar absorption about 95% and low emittance about 0.002% in the infrared band from 2.5 to 15 μm [Fig. 2(c)]. By using 2 mm-thick air gap and polydimethylsiloxane (PDMS) film as a convection blocker and using hydrophobized nanostructured copper-oxide as an effective condensation heat conductor, this device achieved high water-collection rate of 1.063 kg m^{-2} h^{-1} and 70% efficiency of the solar water collection for single-stage solar purification systems.

The above-mentioned spectral designs are all considering that the absorbent surface directly faces the sun, therefore, with a higher temperature than that of the surroundings. However, with a careful structural design, the side surface can be controlled to have a lower temperature, enabling absorption of heat from the ambient to improve the heating effect. In 2018, Li *et al.* designed a cylindrical material consisting of various cotton cores wrapped with plant cellulose with carbon black nanoparticles.[38] In their results, the temperature of the top surface was higher than the ambient due to effective solar absorption, but the side surface had a lower temperature than the ambient. Thus, the environment could act as a hot source relative to the side surface and radiate energy toward it [Fig. 2(d)]. Under this design, the evaporation flux was more than 100% solar-to-vapor energy transfer efficiency which was the traditional limits at the mercy of solar irradiation.

For the past few years, our group also has demonstrated several works on radiative cooling based on polymer materials, which is an emerging passive cooling technology of regulating infrared emissivity. Two kinds of spectral design, including the selective and nonselective ones, are studied.

To achieve a selective emitter in the MIR band, Li *et al.* demonstrated a hierarchically designed polymer nanofiber-based polyethylene oxide (PEO) film by scalable electrostatic spinning process (named as es-PEO) [Fig. 2(e)].[39] Due to the randomly stacked nanofibers with diameter sizes broadly distributed (500–1200 nm, centered at 730 nm), the sunlight could be strongly scattered, especially in the 0.3–1.2 μm wavelength range. It was confirmed by the calculations based on Mie theory together with Chandrasekhar radiative transfer theory. With negligible sunlight absorption of PEO, the reflectivity could reach more than 96% in the solar spectrum. In the MIR band, the absorption (emission) was closely related to various bonding vibrations based on Kirchhoff's law. Fortunately, PEO had C–O–C bond vibrating in 8–13 μm, while C–C bond and C–H bond had weak vibration, so the as-prepared PEO film had high emissivity in 8–13 μm and low emissivity in the other bands. To sum up, the es-PEO film was an ideal selective emitter for all-day radiative cooling. Cooling performance tests show that the cooling temperature could reach 5 °C under the solar intensity of 900 W m^{-2} and the cooling power correspondingly reached 80 W m^{-2}. During nighttime, the es-PEO film also had cooling temperature of 7 °C compared with the ambient and 3 °C cooler than a nonselective emitter. It verified the excellence of the selective radiative emitter in the case of cooling below ambient temperature.

In 2021, Zhu *et al.* introduced the nanoprocessed silk with daytime radiative cooling performance through coupling Al_2O_3 particles to silk with tetrabutyl titanate (TT) [Fig. 2(f)].[40] It improved the reflectivity in the sunlight wavelength range from 86% to 95% and maintained the inherent properties of proteins which had high absorptivity in the whole MIR band. The large difference in the reflective index between Al_2O_3 ($n \approx 1.8$) and the air ($n \approx 1$) resulted in strong scattering of the sunlight. Since Al_2O_3 showed minimum absorption in the UV region, when its nanoparticles had a size of 300 nm, they could achieve high reflectivity in the UV wavelength range. In addition, the reflectivity in the visible-near-infrared (Vis-NIR) band was also enhanced. Finally, the temperature of the nanoprocessed silk was consistently below the ambient during the day and night, even 3.5 °C cooler than that of the ambient under the solar irradiance of 800 W m^{-2}. It had also been observed that the nanoprocessed silk was 8 °C lower compared with that of the natural silk.

IV. THE POSSIBLE SOLUTIONS TO CURRENT PROBLEMS AND THE DIRECTIONS FOR THE FUTURE DEVELOPMENT

Although passive solar heating and radiative cooling based on the spectral design have been developed with very appealing spectroscopic properties, it still remains some questions and challenges.

First, materials in most works appear black or white due to extreme performance, which ignore the needs of specific application scenarios and also have serious esthetic limitations. For example, a transparent glass requires a high transparency in the visible band (0.4–0.7 μm) so as not to affect the normal vision. When it needs cooling, the spectrum is designed to reduce the sunlight transmission in the near infrared band (0.7–2.5 μm) on the basis of high transparency in the visible band. Rho's group designed a transparent radiative cooler based on a dielectric multilayer which could reduce 14.4 °C in an inner space.[41] Similarly, a solar cell requires sunlight that has smaller wavelength than absorption edge, so it needs to reflect the other bands in the solar spectrum in order to minimize the thermal input that may affect the cell performance.[42,43] In addition, considering people's esthetic demand, colorful materials with heating/cooling performance are visually comfortable and more desired including car paints, building design, signals, etc., other than white or black shown by traditional cooling/heating materials.[44] For showing the color, the surface for passive solar heating needs to merely reflect sunlight in the wavelength of corresponding color while absorb sunlight in the wavelength of complementary color for cooling.[45] As Li *et al.* demonstrated, when the surfaces showed a gold color similarly through two different spectra, the visible solar absorption differed between heating material and cooling material by a factor of 3. Therefore, in various scenes, it is necessary to design different materials with corresponding ideal spectrum for visual effect and optimized performance.

Second, spectra in most works cannot change over time, which result in the fact that some materials have no effect or even opposite effect in the process of day-night alternation and summer–winter alternation. One way is designing an appropriate spectrum to reduce the time contradiction between heating and cooling to maximize energy saving. For example, Cui's group regarded the partial heat loss caused by high NIR reflectance as minor in winter in consideration of low solar irradiance, low sun angle, and short daily sunlight time. Thus, they demonstrated colored films with high reflectance in infrared wavelength range for building walls, which could reduce heat gain by 257.6 MJ per area annually by simulation.[46] The emerging method is using phase change materials to change spectral properties so that the surface has more energy out when it is hot and more energy when it is cold. Some works adjust emissivity in the MIR band such as Wu's group and Long's group.[47,48] They all used $W_xV_{1-x}O_2$ as thermal switching, which had metal–insulator transition (MIT) sensitive to temperature. It was transparent to an atmosphere window in 8–13 μm in an insulating state at $T < T_{MIT}$ and absorptive when it was translated into a metallic state at $T > T_{MIT}$. Based on the properties of this material, they designed Fabry–Pérot resonator to enhance contrast and proved good temperature regulation performance for, respectively, roof and window applications. There also exist many works choosing to change absorption and transmission of materials in the solar spectrum, known as thermochromic windows.[49,50] The ideal method is that spectral properties can be regulated in real time with ambient changing, but it is quite challenging to achieve and stays at the level of theoretical calculation.[51,52] Both Wang's group and Lee's group proposed metamaterial with adjustable morphology to change emissivity dynamically. However, the practical sample is fabricated toughly by micro-nanomachining and its morphology change is hardly achieved in actual use. Hence, it is quite significant and necessary to further explore the scalable fabrication of samples with dynamically regulating spectrum. To sum up, materials with dynamic spectral switching are more innovative and more practical in response to actual environmental changes.

In conclusion, it is important to achieve passive solar heating and radiative cooling by effectively harvesting energy from the natural source of the sun and outer space to meet the global sustainability. In this Perspective, we summarize the principles from optical spectrum and propose corresponding ideal designs in different conditions. Under theoretical guidance, several examples of optical spectral design of solar thermal vapor generation and radiative cooling are demonstrated. Remaining challenges and future directions are discussed at the end to guide the future explorations. We believe that the broad application of highly efficient passive solar heating and radiative cooling is an inevitable way for the transformation toward an energy-efficient and sustainable society, and it is now on its way.

ACKNOWLEDGMENTS

We acknowledge the micro-fabrication center at the National Laboratory of Solid State Microstructures (NLSSM) for the technical support. J.Z. acknowledges the support from the XPLORER PRIZE. This work is jointly supported by the National Key Research and Development Program of China (Nos. 2021YFA1400700, 2020YFA0406104, and 2017YFA0205700), the National Natural Science Foundation of China (Nos. 52002168, 12022403, 51925204, 11874211, and 61735008), the Science Foundation of Jiangsu (No. BK20190311), the Key Science and Technology Innovation Program of Shandong Province (No. 2019JZZY020704), the Excellent Research Program of Nanjing University (No. ZYJH005), and the Fundamental Research Funds for the Central Universities (Nos. 021314380184, 021314380190, 021314380140, and 021314380150).

AUTHOR DECLARATIONS

Conflict of Interest

The authors have no conflicts to disclose.

Author Contributions

Yi Jiang: Data curation (equal); Writing – original draft (lead); Writing – review and editing (equal). **Jinlei Li:** Data curation (equal); Writing – original draft (supporting); Writing – review and editing (equal). **Bin Zhu:** Funding acquisition (equal); Project administration (equal); Supervision (equal). **Jia Zhu:** Funding acquisition (equal); Project administration (equal); Supervision (equal).

DATA AVAILABILITY

The data that support the findings of this study are available from the corresponding authors upon reasonable request.

REFERENCES

[1]S. Bilgen, Renewable Sustainable Energy Rev. **38**, 890 (2014).
[2]P. Nejat, F. Jomehzadeh, M. M. Taheri, M. Gohari, and M. Z. A. Majid, Renewable Sustainable Energy Rev. **43**, 843 (2015).
[3]D. Fixsen, Astrophys. J. **707**, 916 (2009).

[4]X. Li, B. Sun, C. Sui, A. Nandi, H. Fang, Y. Peng, G. Tan, and P.-C. Hsu, Nat. Commun. **11**, 1–9 (2020).
[5]S. S. Chandel, S. King, and D. Prasad, in Bringing Solar Down to Earth, Proceedings of ISES, Solar World Congress (2001), p. 183.
[6]S. S. Chandel, Int. Energy J. **7**, 273 (2006).
[7]S. S. Chandel and R. K. Aggarwal, Renewable Energy **33**, 2166 (2008).
[8]S. S. Chandel and A. Sarkar, Energy Build. **86**, 873 (2015).
[9]M. Zeyghami, D. Y. Goswami, and E. Stefanakos, Sol. Energy Mater. Sol. Cells **178**, 115 (2018).
[10]Z. Wang, Y. Liu, P. Tao, Q. Shen, N. Yi, F. Zhang, Q. Liu, C. Song, D. Zhang, W. Shang, and T. Deng, Small **10**, 3234 (2014).
[11]H. Ghasemi, G. Ni, A. M. Marconnet, J. Loomis, S. Yerci, N. Miljkovic, and G. Chen, Nat. Commun. **5**, 4449 (2014).
[12]R. Hu, Y. Liu, S. Shin, S. Huang, X. Ren, W. Shu, J. Cheng, G. Tao, W. Xu, R. Chen, and X. Luo, Adv. Energy Mater. **10**, 1903921 (2020).
[13]F. J. Zhu and Q. Q. Feng, Int. J. Therm. Sci. **165**, 106899 (2021).
[14]C. Granqvist and A. Hjortsberg, J. Appl. Phys. **52**, 4205 (1981).
[15]P. Tao, G. Ni, C. Song, W. Shang, J. Wu, J. Zhu, G. Chen, and T. Deng, Nat. Energy **3**, 1031 (2018).
[16]L. Zhou, X. Li, G. W. Ni, S. Zhu, and J. Zhu, Nat. Sci. Rev. **6**, 562 (2019).
[17]A. Lenert and E. N. Wang, Sol. Energy **86**, 253 (2012).
[18]N. J. Hogan, A. S. Urban, C. Ayala-Orozco, A. Pimpinelli, P. Nordlander, and N. J. Halas, Nano Lett. **14**, 4640 (2014).
[19]A. P. Raman, M. Abou Anoma, L. Zhu, E. Rephaeli, and S. Fan, Nature **515**, 540 (2014).
[20]P.-C. Hsu, A. Y. Song, P. B. Catrysse, C. Liu, Y. Peng, J. Xie, S. Fan, and Y. Cui, Science **353**, 1019 (2016).
[21]J. Mandal, Y. Fu, A. C. Overvig, M. Jia, K. Sun, N. N. Shi, H. Zhou, X. Xiao, N. Yu, and Y. Yang, Science **362**, 315 (2018).
[22]Y. Zhai, Y. Ma, S. N. David, D. Zhao, R. Lou, G. Tan, R. Yang, and X. Yin, Science **355**, 1062 (2017).
[23]E. Rephaeli, A. Raman, and S. Fan, Nano Lett. **13**, 1457 (2013).
[24]X. Yin, R. Yang, G. Tan, and S. Fan, Science **370**, 786 (2020).
[25]G. Xiao, X. Wang, M. Ni, F. Wang, W. Zhu, Z. Luo, and K. Cen, Appl. Energy **103**, 642 (2013).
[26]J. R. Werber, C. O. Osuji, and M. Elimelech, Nat. Rev. Mater. **1**, 16018 (2016).
[27]T. Tong and M. Elimelech, Environ. Sci. Technol. **50**, 6846 (2016).
[28]N. Xu, J. Li, Y. Wang, C. Fang, X. Li, Y. Wang, L. Zhou, B. Zhu, Z. Wu, S. Zhu, and J. Zhu, Sci. Adv. **5**, eaaw7013 (2019).
[29]G. Xue, Y. Xu, T. Ding, J. Li, J. Yin, W. Fei, Y. Cao, J. Yu, L. Yuan, L. Gong, J. Chen, S. Deng, J. Zhou, and W. Guo, Nat. Nanotechnol. **12**, 317 (2017).
[30]P. Yang, K. Liu, Q. Chen, J. Li, J. Duan, G. Xue, Z. Xu, W. Xie, and J. Zhou, Energy Environ. Sci. **10**, 1923 (2017).
[31]L. Zhou, Y. Tan, D. Ji, B. Zhu, P. Zhang, J. Xu, Q. Gan, Z. Yu, and J. Zhu, Sci. Adv. **2**, e1501227 (2016).
[32]L. Zhou, Y. Tan, J. Wang, W. Xu, Y. Yuan, W. Cai, S. Zhu, and J. Zhu, Nat. Photonics **10**, 393 (2016).
[33]L. Zhou, S. Zhuang, C. He, Y. Tan, Z. Wang, and J. Zhu, Nano Energy **32**, 195 (2017).
[34]X. Li, W. Xu, M. Tang, L. Zhou, B. Zhu, S. Zhu, and J. Zhu, Proc. Natl. Acad. Sci. **113**, 13953 (2016).
[35]X. Hu, W. Xu, L. Zhou, Y. Tan, Y. Wang, S. Zhu, and J. Zhu, Adv. Mater. **29**, 1604031 (2017).
[36]N. Xu, X. Hu, W. Xu, X. Li, L. Zhou, S. Zhu, and J. Zhu, Adv. Mater. **29**, 1606762 (2017).
[37]F. Wang, N. Xu, W. Zhao, L. Zhou, P. Zhu, X. Wang, B. Zhu, and J. Zhu, Joule **5**, 1602 (2021).
[38]X. Li, J. Li, J. Lu, N. Xu, C. Chen, X. Min, B. Zhu, H. Li, L. Zhou, S. Zhu, T. Zhang, and J. Zhu, Joule **2**, 1331 (2018).
[39]D. Li, X. Liu, W. Li, Z. Lin, B. Zhu, Z. Li, J. Li, B. Li, S. Fan, J. Xie, and J. Zhu, Nat. Nanotechnol. **16**, 153 (2021).
[40]B. Zhu, W. Li, Q. Zhang, D. Li, X. Liu, Y. Wang, N. Xu, Z. Wu, J. Li, X. Li, P. B. Catrysse, W. Xu, S. Fan, and J. Zhu, Nat. Nanotechnol. **16**, 1342 (2021).
[41]M. Kim, D. Lee, S. Son, Y. Yang, H. Lee, and J. Rho, Adv. Opt. Mater **9**, 2002226 (2021).
[42]L. Zhu, A. P. Raman, and S. Fan, Proc. Natl. Acad. Sci. **112**, 12282 (2015).
[43]W. Li, Y. Shi, K. Chen, L. Zhu, and S. Fan, ACS Photonics **4**, 774 (2017).
[44]R. A. Yalc¸ın, E. Blandre, K. Joulain, and J. Drévillon, ACS Photonics **7**, 1312 (2020).
[45]W. Li, Y. Shi, Z. Chen, and S. Fan, Nat. Commun. **9**, 4240 (2018).
[46]Y. Peng, L. Fan, W. Jin, Y. Ye, Z. Huang, S. Zhai, X. Luo, Y. Ma, J. Tang, J. Zhou, L. C. Greenburg, A. Majumdar, S. Fan, and Y. Cui, Nat. Sustainable **5**, 339 (2022).
[47]K. Tang, K. Dong, J. Li, M. P. Gordon, F. G. Reichertz, H. Kim, Y. Rho, Q. Wang, C.-Y. Lin, C. P. Grigoropoulos, A. Javey, J. J. Urban, J. Yao, R. Levinson, and J. Wu, Science **374**, 1504 (2021).
[48]S. Wang, T. Jiang, Y. Meng, R. Yang, G. Tan, and Y. Long, Science **374**, 1501 (2021).
[49]M. Kamalisarvestani, R. Saidur, S. Mekhilef, and F. Javadi, Renewable Sustainable Energy Rev. **26**, 353 (2013).
[50]I. P. Parkin and T. D. Manning, J. Chem. Educ. **83**, 393 (2006).
[51]A. Krishna and J. Lee, Nanoscale Microscale Thermophys. Eng. **22**, 124 (2018).
[52]W. Wang, Z. Zhao, Q. Zou, B. Hong, W. Zhang, and G. P. Wang, J. Mater. Chem. C **8**, 3192 (2020).